Received: 26 January 2024 | Revised: 21 April 2024 | Accepted: 24 April 2024

DOI: 10.1111/gcbb.13170

Global Change Biology Bioenergy
BIOPRODUCTS FOR A SUSTAINABLE BIOECONOMY

WILEY

RESEARCH ARTICLE

A critical re-analysis of biochar properties prediction from production parameters and elemental analysis

Johanne Lebrun Thauront[1] | **Gerhard Soja**[2,3] | **Hans-Peter Schmidt**[4] | **Samuel Abiven**[1,5]

[1]Laboratoire de Géologie, École Normale Supérieure-PSL, CNRS, IPSL, Paris, France

[2]University of Natural Resources and Life Sciences, IVET/BOKU, Wien, Austria

[3]AIT Austrian Institute of Technology GmbH, Tulln, Austria

[4]Ithaka Institute for Carbon Strategies, Arbaz, Switzerland

[5]CEREEP-Ecotron Île-de-France, École Normale Supérieure-PSL, CNRS, Saint-Pierre-Lès-Nemours, France

Correspondence
Johanne Lebrun Thauront, Laboratoire de Géologie, École Normale Supérieure-PSL, CNRS, IPSL, 24 rue Lhomond, Paris 75005, France.
Email: johanne.lebrun.thauront@ens.psl.eu

Funding information
Centre National de la Recherche Scientifique

Abstract

Biochar is the product of intentional pyrolysis of organic feedstocks. It is made under controlled conditions in order to achieve desired physico-chemical characteristics. These characteristics ultimately affect biochar properties as a soil amendment. When biochar is used for carbon storage, an important property is its persistence in soil, often described by the proportion of biochar carbon remaining in soil after a 100 years (F_{perm}). We analyzed published data on 1230 biochars to re-evaluate the effect of pyrolysis parameters on biochar characteristics and the possibility to predict F_{perm} from the maximum temperature reached during pyrolysis (HTT). We showed that biochar ash and nitrogen (N) contents were mostly affected by feedstock type. The oxygen to carbon (O:C) and hydrogen to carbon (H:C) ratios were mostly affected by the extent of pyrolysis (a combination of HTT and pyrolysis duration), except for non (ligno)cellulosic feedstocks (plastic waste, sewage sludge). The volatile matter (VM) content was affected by both feedstock type and the extent of pyrolysis. We demonstrated that HTT is the main driver of H:C -- an indicator of persistence -- but that it is not measured accurately enough to precisely predict H:C, let alone persistence. We examined the equations to estimate F_{perm} available in the literature and showed that F_{perm} calculated from HTT presented little agreement with F_{perm} calculated from H:C. The sign and magnitude of the bias depended on the equation used to calculate F_{perm} and the dispersion was usually large. This could lead to improper compensation of carbon emissions and wrong reporting of carbon sinks in national carbon accounting schemes. We recommend not to use HTT as a predictor for persistence and stress the importance to rapidly develop more accurate proxies of biochar C persistence in soil.

KEYWORDS

carbon accounting, carbon sink, highest treatment temperature, persistence, prediction, ultimate analysis

Hans-Peter Schmidt and Samuel Abiven should be considered joint senior authors.

1 | INTRODUCTION

Biochar is the carbonaceous solid residue of intentional pyrolysis of organic materials such as wood, crop residues, manure, or sewage sludge. Its long persistence in soils, from centuries to millennia (Bowring et al., 2022; Singh, Abiven, et al., 2012) makes it a good candidate for carbon sequestration in a climate mitigation perspective (Gaunt & Cowie, 2009). Its addition to agricultural soils can increase crop yield and soil quality via increased water retention and nutrient exchange capacity, direct nutrient provision, and soil biota stimulation (Crane-Droesch et al., 2013; Schmidt et al., 2021). It can also be used as sorbent for a large range of organic and inorganic contaminants due to its high surface area, varying surface functional groups and polarity (Chun et al., 2004; Harvey et al., 2011; Hassan et al., 2020). Biochar physico-chemical characteristics vary with the extent of pyrolysis (i.e. the degree to which the pyrolysis reactions proceeded; Keiluweit et al., 2010; Ronsse et al., 2013; Wurster et al., 2013) and the nature of the feedstock from which it was produced (Hassan et al., 2020; Ippolito et al., 2020; Mukome et al., 2013; Qiu et al., 2015; Zhang et al., 2017). The term biochar thus encompasses material with highly variable characteristics. Biochar properties result from the interaction of these characteristics with its environment and it is important to choose or produce the right biochar for the right application (Abiven et al., 2014; Enders et al., 2012; Ippolito et al., 2020; Novak et al., 2009; Sohi et al., 2015; Xiao et al., 2018). In this regard, the heterogeneous quality of biochar products is one of the key challenges faced by end users and policy makers. In addition, biochar has to go through a certification procedure in order to provide a reliable product, so there is an urgent need to define accurate and repeatable analytical methods to do so.

These issues are addressed using different approaches. On the one hand, in-depth investigations based on (high resolution) mass spectrometry, nuclear magnetic resonance (NMR), various spectroscopies (FTIR, Raman, XPS, NEXAFS, etc.), scanning electron microscopy, and X-ray diffraction reveal the complexity of biochar chemistry and structure (Amin et al., 2016; Brewer et al., 2014; Budai et al., 2013; Keiluweit et al., 2010; Moško et al., 2021; Wiedemeier et al., 2015; Wurster et al., 2013; Xiao et al., 2018) and how it affects its properties (Brewer et al., 2012; Chun et al., 2004; de la Rosa et al., 2014; Fan et al., 2020; Harvey et al., 2011; Singh, Cowie, et al., 2012; Sun et al., 2013; Wei et al., 2017). On the other hand, efforts have been made to relate simple physico-chemical characteristics of biochar to properties relevant to various applications. Those simpler analytical methods are usually divided in two categories, ultimate analysis—which consist of determining the elemental composition of biochar (all or a subset of carbon C, hydrogen H, oxygen O, nitrogen N and sulphur S content)—and proximate analysis—which distinguishes residual moisture (adsorbed water), volatile matter (VM, matter lost upon re-heating in oxygen limited conditions), ash (mineral matter remaining after combustion), and fixed C (the rest of the biochar matter) (Budai et al., 2013). However, ultimate and proximate analyses are not easily accessible in the field and not available in all laboratories. Some authors have taken it one step further, suggesting to directly derive biochar properties from production parameters such as pyrolysis conditions and feedstock type (IPCC, 2019; Woolf et al., 2021). In this study, we question the validity of such approach, with a particular focus on the estimation of biochar carbon persistence in soils.

Carbon dioxide removal has been identified as a necessary step in most climate mitigation scenarios permitting to stay below 2.0°C of global warming (IPCC, 2023). Since 2003, countries that are party to the United Nation Framework Convention on Climate Change are requested to submit regularly National Inventories of greenhouse gases (GHGs) emissions, including positive and negative emissions of GHGs due to land use. If any form of carbon storage in soil is to be included in carbon markets and carbon inventories, an accurate and precise estimate of carbon sequestration from various land-use related practices is needed. In the case of biochar, accounting for carbon sequestration requires to know, among other parameters, its persistence in soils at relevant time-scales (e.g. persistence over a 100 years for C-sink markets; Budai et al., 2013; IPCC, 2019; Woolf et al., 2021).

Biochar stability in soil increases with decreasing oxygen-to-carbon ratio (O:C) (Spokas, 2010; less oxygen bearing reactive groups), decreasing hydrogen-to-carbon ratio (H:C) (Enders et al., 2012; less C-H bonds means increased connectivity of the carbonaceous skeleton i.e. increased aromaticity and condensation; Wiedemeier et al., 2015) and decreasing ratios of volatile to fixed C (volatiles are made of more labile compounds that will be quickly degraded upon biochar addition to soil) (Crombie et al., 2013; Spokas, 2010; Yuan et al., 2014; Zimmerman, 2010). The more aromatic and condensed the biochar, the harder it is for (micro)organisms to oxidize the pyrogenic carbon molecules and break the chemical bonds holding them together. Budai et al. (2013) and Camps Arbestain et al. (2015) suggested that a biochar with H:C ratio<0.4 has an average degradation rate of 0.3% per year. Woolf et al. (2021) proposed a simple formula linking H:C and persistence that they recommend using preferentially over production parameters based estimates of persistence in soil when elemental analysis is available. Azzi et al. (2024) recently expanded and systematized this work.

Highly aromatic and condensed biochar (low H:C) with little surface reactivity (low O:C) is obtained through high pyrolysis temperature and long residence times in the pyrolyser which promote more complete conversion of cellulose, hemi-cellulose, and lignin into reduced, polyaromatic carbon (Anca-Couce, 2016; Antal & Grønli, 2003; Janu et al., 2021; Keiluweit et al., 2010; Ronsse et al., 2013; Wiedemeier et al., 2015). Pyrolysis temperature has been shown to be one of the most influential parameters in determining stability (Fang et al., 2019, 2014; Liu et al., 2020; Zimmerman, 2010). On this basis, in the latest update of their Guidelines for National Greenhouse Gas Inventories, the IPCC (2019) estimates the fraction of biochar remaining in soil after a 100 years (F_{perm}) at 89% for highest treatment temperatures (HTT, the maximum temperature reached during pyrolysis) of more than 600°C, 80% for HTT comprised between 450 and 600°C and 65% for HTT between 350 and 450°C. Woolf et al. (2021) recently updated these values to 82%, 71%, and 63% respectively, based on an expanded dataset. However, if for each given temperature series (see SI bibliography table for a list of references) biochar characteristics vary systematically, the relation becomes less clear when many studies are considered together. This is clearly visible in the figures from Ippolito et al. (2020), who gathered data from over 5000 studies representing 50,000 individual biochars. Indeed, pyrolysis is a complex process involving many different reactants (usually cellulose, hemicellulose, lignin, and mineral elements) going through primary and secondary reactions to form many products (chars, condensable volatiles, and gases). The use of different pyrolysis technologies, operating in batch or continuous conditions, with widely different particle sizes, heating rates and residence times, adds to this complexity. Despite repeated warnings in book chapters (Lehmann & Joseph, 2009; Steiner, 2016), editor's note (Cayuela et al., 2022), and research articles (Rathnayake et al., 2020) that HTT is not trivial to measure and is not sufficient to characterize biochar, new studies still suggest to use HTT for predicting biochar characteristics and properties (Leng et al., 2022; Palansooriya et al., 2022), such as persistence in soils.

In this work, we check the hypothesis that using production parameters instead of physico-chemical characteristics to predict biochar properties is an inherent source of uncertainty and leads to poor predictions. To do so we gathered and re-analyzed published data ($n = 1230$ biochars) on biochar production and its physico-chemical characteristics and investigated the precision of predictions of chemical characteristics and persistence from production parameters, in particular the highest treatment temperature.

2 | MATERIALS AND METHODS

2.1 | Data collection

We searched the Scopus electronic database using the terms "biochar properties" AND "biochar characteristics" in titles, abstracts, and keywords and restricted the results to journal articles until 2021. Based on title and abstract, we excluded studies that were not in English, that were exclusively about biochar application (and not biochar production), that were about hydrothermally produced char, and where biochar was produced using inorganic additives because of too few observations to allow meaningful comparisons. We accessed the full text of all selected articles and additionally rejected the ones that did not include at least HTT, H and C content or H:C molar (atomic) ratio, that did not report original biochar data, or where a description of the biochar production method was missing. Articles listed in one review (Hassan et al., 2020) which provided H, C, and HTT data were accessed individually to collect details of production methods that were not reported in the review, and submitted to the same exclusion criteria. This systematic literature search resulted in the selection of 137 studies (see Figure S1 for a detailed account of the data selection process). Data were extracted manually from tables in the main text, supplementary information, or separately published dataset. Data reported only in figures (two studies) were not extracted, as data extraction from figures may introduce an additional uncertainty in the reported values.

We collected the following data: production parameters relative to pyrolysis (HTT, heating rate, and pyrolysis duration, that is the time the feedstock is held at HTT, sometimes called residence time) and feedstock (nature of the feedstock and particle size grouped in three size classes, smaller than 1 mm, smaller than 1 cm and 1 cm or larger for the largest typical dimension), biochar yield, proximate (VM, ash, and fixed C content) and ultimate chemical characteristics (total C, H, O, N, and S content as well as organic C (C_{org}) content where available). All proximate and ultimate characteristics were registered as weight percentage on a dry mass basis (wt% db); if they were reported in another way (dry, ash free basis, wt% daf, for instance) they were recalculated where possible or discarded otherwise (three studies). H:C, O:C and H:C_{org} molar ratios were recalculated from the H, C, C_{org} and O data when available according to Equation (1),

$$\mathrm{X{:}\,C_{molar}} = \frac{\mathrm{X(wt\,\%\,db)} / \mathrm{M_X}}{\mathrm{C(wt\,\%\,db)} / 12.011}, \quad (1)$$

where X stands for O or H and M_X for their respective standard atomic weight in $g\,mol^{-1}$. Pyrolysis type was taken as reported by the authors.

We discarded data that failed at a plausibility check based on the following two criteria: (i) Observations for which H:C molar ratio was greater than 3 were removed as it is impossible for complex organic material to have such a high H:C ratio. A measured H:C ratio above 3 can only be the result of an important contribution of mineral hydroxides (in ashes) or a very large residual moisture increasing the H content measured by elemental analysis, or an analytical error. (ii) Observations for which the sum of ash, C, H, O, N, and S (or a subset of these) was higher than 110% were excluded as we considered that an overall analytical error of more than 10% was not acceptable. In order to compare our results with the observations of Woolf et al. (2021) and the IPCC (2019), we also discarded biochars produced at HTT below 350°C, although there is no consensus on this limit. Pyrolysis reactions can occur at temperatures as low as 300°C (Antal & Grønli, 2003), but major changes in the composition and properties of the material usually occur at higher temperatures (Keiluweit et al., 2010). The European Biochar Certificate (EBC, 2022) sets a minimum pyrolysis temperature of 350°C so that a material can be certified as biochar. Overall, 30% of the entries were discarded based on these plausibility criteria, the final dataset consist of 1230 entries from 129 studies.

We grouped feedstocks in eight feedstock types. (1) Woody (Wo) feedstock encompasses all biochar produced from aboveground parts of trees and bushes except leaves. (2) Herbaceous (H) feedstock consists of leaves, and stems of non-woody plants. (3) Shells and kernels (S&K) comprise the stone or pit of fruits, nutshells, cereal husks and corncobs. (4) Manure (M) designates livestock litter and manure, mixed or not with straw or wood dust. (5) Sewage sludge (SS) includes the leftover slurry of water treatment plants. (6) Cellulosic waste (C waste) comprises cardboard and paper, fabric from natural fibres, as well as the residue from paper production. (7) Non-cellulosic waste (NC waste) includes plastics, synthetic fabrics and mixed household wastes with 50% or more synthetic material. (8) Kitchen waste (K waste) was distinguished from other plant-based feedstocks as it may contain non-plant material such as bones and fish-bones, may have a high salt content and because part of the initial plant biomass may have been transformed already by cooking. The number of entries per feedstock type is reported in Table S1. The complete dataset and associated bibliography are available online (Lebrun Thauront et al., 2024).

2.2 | Data analysis

Data analyses were carried out using R version 4.0.5 (R Core Team, 2021), Rstudio (RStudio, 2021) and the packages tidyverse (Wickham et al., 2019), Hmisc (Harrell, 2023), cowplot (Wilke, 2020), ggfortify (Horikoshi et al., 2018; Tang et al., 2016), corrplot (Wei & Simko, 2021), MASS (Venables & Ripley, 2002), WRS (Wilcox & Schönbrodt, 2014), boot (Canty & Ripley, 2022; Davinson & Hinkley, 1997), lme4 (Bates et al., 2015), and ciTools (Haman & Avery, 2020). All statistical tests were carried out at the 95% confidence level.

We used boxplot to visualize central tendency and quartiles of grouped observations while violin-plots allowed for a better visualization of the distribution of observations. The non-parametric Wilcoxon-Mann–Whitney test was used to compare the distribution location of two groups when observations were not normally distributed. We used the non-parametric Spearman's rank correlation coefficient and the Fisher's F-test to assess the strength and significance of correlations between variables respectively. Correlations between pairs of variables were calculated across all non-missing pairs of observations in the dataset. For multiple pairwise comparisons *p*-values were adjusted using the Holm–Bonferroni correction. We used principal components analysis (PCA) to visualize correlation between proximate and ultimate variables in the data set and identify the underlying information. PCA was performed on centered and scaled variables. Extra variables can be represented in the principal components (PCs) space even if they are not included in the PCA. The correlation coefficient of the extra variable with each represented PCs gives its position in the biplot (plot of variables and individual data points in the PC space). When evaluating the prediction of H:C from HTT, we fitted various linear regression models to the data and compared the quality of regression using residual standard error (S), adjusted R^2 and visual examination of residual, normal Q–Q and leverage plots in order to choose the appropriate model. We tested that the coefficients of the linear regressions were statistically different from 0 using Student's *t*-test and the overall significance of the regressions with Fisher's *F*-test. To robustly fit data showing high leverage points and outliers and compare regression coefficients between feedstock types, we used Theil-Sen estimator and bootstrap confidence intervals and hypothesis test since data were clearly heteroskedastic and non-normally distributed (Moses & Klockars, 2009; Wilcox, 1998; Wilcox & Clark, 2013). To account for non-independence in the data (data from within the same study are likely to present a better correlation than between studies), we used publication ID as a random effect in linear mixed models.

2.3 | Persistence estimates

The fraction of biochar carbon remaining in the soil after 100 years was calculated from H:C ($F_{perm,H:C}$) and from HTT ($F_{perm,HTT}$) using the formula from Woolf et al. (2021) for a world average soil temperature of 14.9°C (Equations 2 and 3) and from the IPCC (2019) (Equation 4). Rodrigues et al. (2023) and Azzi et al. (2024) recently proposed new equations for $F_{perm,H:C}$ (Table S2) but in the absence of a clear indication as to which is preferred we use the equation from Woolf et al. (2021) as an example. We also calculated ΔF_{perm} the difference between $F_{perm,H:C}$ and $F_{perm,HTT}$ (Equation 5)

$$F_{perm,H:C} = 1.04 + 0.635H:C, \quad (2)$$

$$F_{perm,HTT} = \begin{cases} 0.63 \text{ if } HTT \in [350;450[\,^{\circ}C \\ 0.71 \text{ if } HTT \in [450;600[\,^{\circ}C \\ 0.82 \text{ if } HTT \geq 600\,^{\circ}C \end{cases}, \quad (3)$$

$$F_{perm,HTT} = \begin{cases} 0.65 \text{ if } HTT \in [350;450[\,^{\circ}C \\ 0.80 \text{ if } HTT \in [450;600[\,^{\circ}C \\ 0.89 \text{ if } HTT \geq 600\,^{\circ} \end{cases}, \quad (4)$$

$$\Delta F_{perm} = F_{perm,H:C} - F_{perm,HTT}. \quad (5)$$

3 | RESULTS AND DISCUSSION

3.1 | Overview of the database—biochar characteristics

Data were collected cover a wide range of pyrolysis conditions and feedstock types, resulting in biochars with diverse chemical characteristics (Table 1).

HTT ranges from 350 to 1000°C, with a median of 500°C. Pyrolysis duration (i.e. holding time at HTT) ranges from a few seconds to 4 days. Feedstock particle size ranges from micrometers to several tens of centimeters. This large spread in pyrolysis conditions likely reflects the diversity of pyrolysis technology used, from traditional kilns (Tintner et al., 2020) to continuous fluidized bed reactors (Brewer et al., 2009, 2012; Cheah et al., 2014; Kim et al., 2012; Lee et al., 2010). We did not attempt to group biochars by pyrolysis type since the definitions of slow, fast and flash pyrolysis and gasification vary from study to study. As per the declaration of the original authors, 87% of biochars were made by slow pyrolysis.

We observed only weak or no correlation among pyrolysis parameters (Table S3). Independent of the production technology, we would expect a positive correlation between pyrolysis duration and particle size

TABLE 1 Biochar production parameters, proximate and ultimate characteristics.

	HTT[a] (°C)	Pyrolysis duration (min)	Heating rate (°C min^{-1})
Production parameters			
Min	350	0	1.67
Q1	400	30	8
Median	500	60	10
Q3	600	120	50
Max	1000	5760	100
	VM[b] wt% db[d]	**Fixed C[c] wt% db**	**Ash wt% db**
Proximate chemical characteristics			
Min	0.922	2.1	0.05
Q1	14.3	35.555	4.3475
Median	28	52.04	12.245
Q3	44.25	66.865	26.11
Max	95.1	95.04	89.9
	C_{org}[e] wt% db	**C wt% db**	**H wt% db**
Ultimate chemical characteristics			
Min	11.2	1.05	0.03
Q1	65.8	50	1.64
Median	73.6	66.32	2.66
Q3	79.675	76.18	3.77
Max	91.1	98.8	13
	O wt% db	N wt% db	S wt% db
Min	0.01	0.01	0.00116
Q1	8.42	0.3	0.06
Median	13.2	0.7	0.129
Q3	19	1.4	0.265
Max	64.87	21.8	81
	H:C	**H:C_{org}**	**O:C**
Molar ratios			
Min	0.01	0.206	0.01
Q1	0.31	0.35875	0.09
Median	0.51	0.431	0.15
Q3	0.74	0.5825	0.24
Max	2.8	1.82	1.66

Note: Descriptive statistics: Min, minimum; Q1, first quartile; Q3, third quartile; Max, maximum.

[a]Highest treatment temperature.

[b]Volatile matter.

[c]Fixed carbon (calculated by difference).

[d]Weight percent dry mass basis.

[e]Organic carbon.

and between pyrolysis duration and HTT to overcome the heat transfer and kinetic limitations (Koufopanos et al., 1991; Park et al., 2010; Simmons & Gentry, 1986). Kinetic limitations arise when reaction rates are slow compared to pyrolysis duration. As temperature increases reaction rates increase so that a shorter pyrolysis duration is needed to reach a similar extent of pyrolysis. Heat transfer limitation arises when the rate of heat propagation through the oven and feedstock particles volume is slow compared to the pyrolysis duration. If the particle size increases and the temperature gradient decreases (lower HTT and/or slower heating rate) the time needed for the heat to reach the core of the particle increases and a longer pyrolysis duration is needed to reach a similar extent of pyrolysis throughout the material. To ensure reproducibility and predictability of biochar characteristics and properties, all production parameters should be reported which is not the case in 51% of the publications analyzed here.

The volatile matter content of all biochars ranged from 14.3 wt% db (first quartile Q1) to 44.25 wt% db (third quartile Q3). VM was highly variable within each feedstock type (Figure 1a and Table S4), which resulted in almost no significant differences between feedstock types. VM tended to be higher for biochars derived from woody and shells and kernels feedstocks and lower for herbaceous, kitchen waste and sewage sludge feedstocks. A moderate dependency of VM on feedstock type was previously reported (Askeland et al., 2019; Cantrell et al., 2012; Khajavi-Shojaei et al., 2020; Mašek et al., 2018; Suman & Gautam, 2017) but it should be remarked that VM was not measured consistently from one study to another. VM is measured as the mass loss between 105°C and a variable upper limit, most often 950°C, in a closed crucible. The maximum temperature and holding time at that temperature vary with national norm or local procedure that researchers follow. We found VM determination temperatures ranging from 350 to 950°C. Moreover, VM content

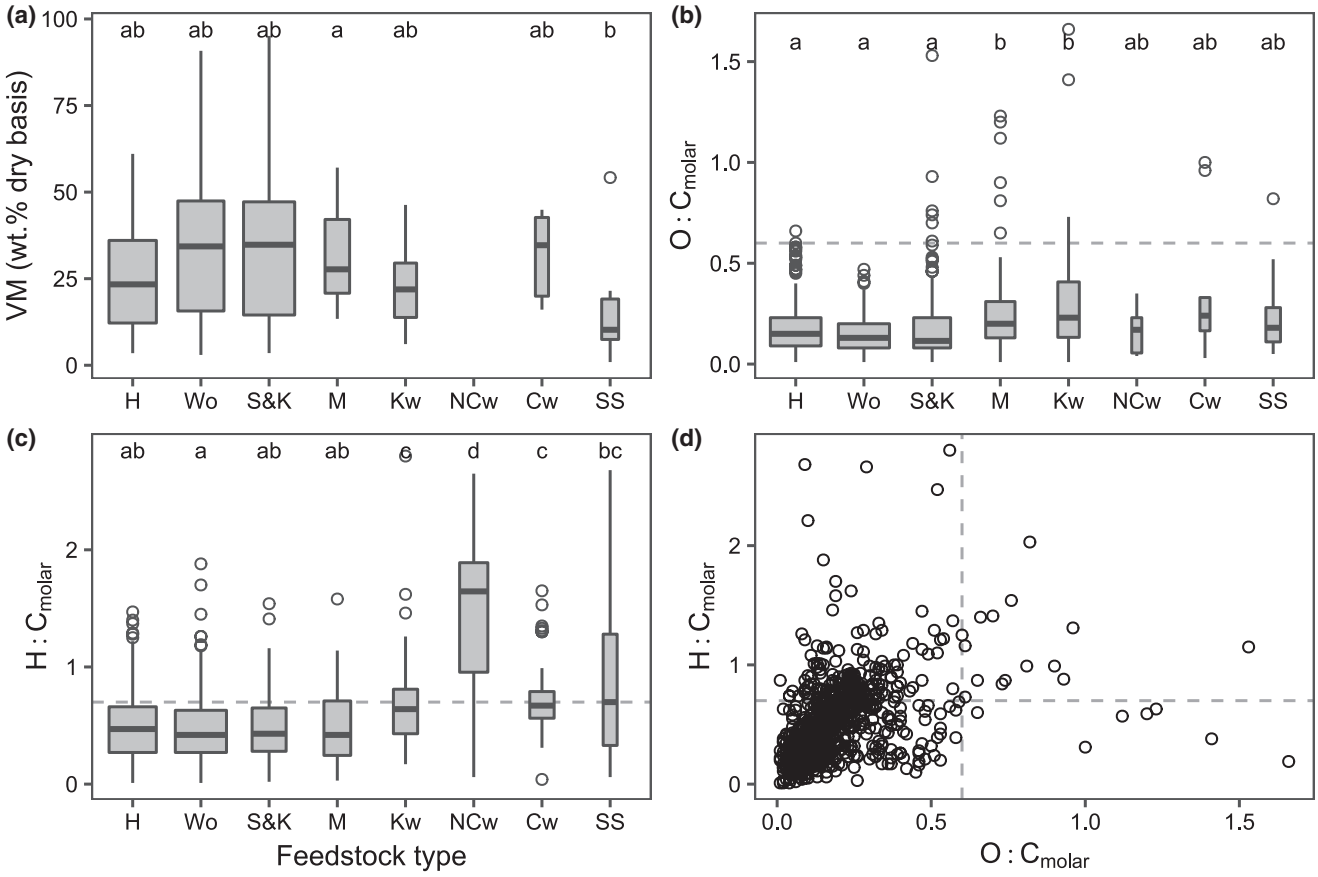

FIGURE 1 Boxplot of (a) volatile matter content, (b) O:C molar ratio (the dashed line at 0.6 shows the O:C value below which biochars have a half-life in soil of more than 100 years according to Spokas, 2010), (c) H:C molar ratio, (the dashed line at H:C = 0.7 shows the EBC (2022) and IBI (Budai et al., 2013) limit for a material to qualify as biochar), by feedstock type (H—herbaceous, Wo—woody, S&K—shells and kernels, M—manure, Kw—kitchen waste, NCw—non-cellulosic waste, Cw—cellulosic waste, SS—sewage sludge). The width of the box is proportional to the number of observations. Feedstock types sharing a letter do not differ significantly at the 95% confidence level according to the Wilcoxon–Mann–Whitney test. (d) Van Krevelen diagram, the dashed lines are as per panels (b) and (c).

is likely sensitive to cool down procedure and duration of storage before analysis (Spokas, 2010).

The median O:C molar ratio (Figure 1b and Table S4) was 0.15 (Q1–Q3 = 0.09–0.24). Herbaceous, woody and shells and kernels derived biochars had lower O:C ratio (median = 0.15, 0.13 and 0.115, Q1–Q3 = 0.09–0.23, 0.08–0.2 and 0.08–0.23 respectively) than manure and kitchen waste derived biochars (median = 0.2 and 0.23, Q1–Q3 = 0.13–0.31 and 0.1325–0.4075 respectively). It suggests an inherited effect of raw biomass chemical composition on O:C, possibly due to the formation of different products during pyrolysis of compounds with high O content, as discussed in Uchimiya et al. (2011) and references therein. On the contrary, other authors found no significant differences between O:C of biochars produced from 4 different feedstocks (Mukome et al., 2013; Zhang et al., 2017). Crombie et al. (2013) and Campos et al. (2020) noted that O:C varied more from one feedstock to another than H:C, which we don't observe here. Janu et al. (2021) showed that the difference of spectral features related to O containing functional groups between different feedstock tend to disappear at higher temperatures. The oxygen to carbon (O:C) ratio is associated with high measurement uncertainty because O content is most often not directly measured but calculated by subtracting C, H, N, S and ash content from 100% of the mass, as discussed by others (Budai et al., 2014; Enders et al., 2012). In particular, ash measurement suffers from biases that will pass on O. Ash is measured as the mass of the material remaining after combustion. The combustion temperature and holding time at that temperature vary with the national norm or local procedure that researchers follow, yielding different results. Among the articles analyzed here we found ash determination temperatures ranging from 400 to 1000°C, 750°C being the most commonly used temperature. Depending on the oxidation temperature during ash analysis, minerals may oxidize increasing the mass of ash and decreasing the calculated mass of O, or volatilize, decreasing the mass of ash and increasing the calculated mass of O (Bachmann et al., 2016).

The median H:C molar ratio (Figure 1c and Table S4) was 0.51 (Q1–Q3 = 0.31–0.74). NC-waste derived biochars had the highest H:C (median = 1.64, Q1–Q3 = 0.96–1.89), sewage sludge (median = 0.7, Q1–Q3 = 0.33–1.28), C-waste (median = 0.67, Q1–Q3 = 0.56–0.79), and K-waste (median = 0.64, Q1-Q3 = 0.43–0.81) derived biochars showed intermediate H:C while plant and manure derived biochars had the lowest H:C (median = 0.47, 0.42, 0.43 and 0.42, Q1–Q3 = 0.27–0.66, 0.27–0.63, 0.28–0.65 and 0.25–0.71 for herbaceous, woody, shells and kernels and manure, respectively). Uncertainties affecting H measurement are discussed later.

The Van Krevelen plot in Figure 1d shows the dispersion of H:C and O:C values across feedstock types. 29% of all entries fall outside the EBC (2022) and International Biochar Initiative (IBI; Budai et al., 2013) limits to be considered as biochar (H:C < 0.7 and O:C < 0.6, lower left corner of the plot), this number goes up to 63% if we consider only biochars produced at HTT ≤ 400°C and to 84% for NC-waste derived biochars. A large part of the materials presented as biochar by the scientific community in research studies does not meet the thresholds that define biochar for industrial production and environmental application.

3.2 | Relation of proximate and ultimate characteristics of biochars to pyrolysis parameters and feedstock type

Figure 2 represents the first two PCs of a PCA carried out on 252 entries for which we had observations for all of H:C, O:C, ash, VM and N content. It shows that more than 70% of the total variance (Figure S2) in the dataset can be explained by the extent of pyrolysis (PC1)—driven by HTT—and a feedstock type effect (PC2).

H:C, O:C and VM were the main contributors to PC1 (Figure 2, loadings of +0.63, +0.62 and +0.42 respectively, Table S5). We interpret this PC as representing the extent to which the pyrolysis reactions proceeded towards the formation of more aromatic, condensed (low H:C) (Wiedemeier et al., 2015) and reduced (low O:C) (Brewer

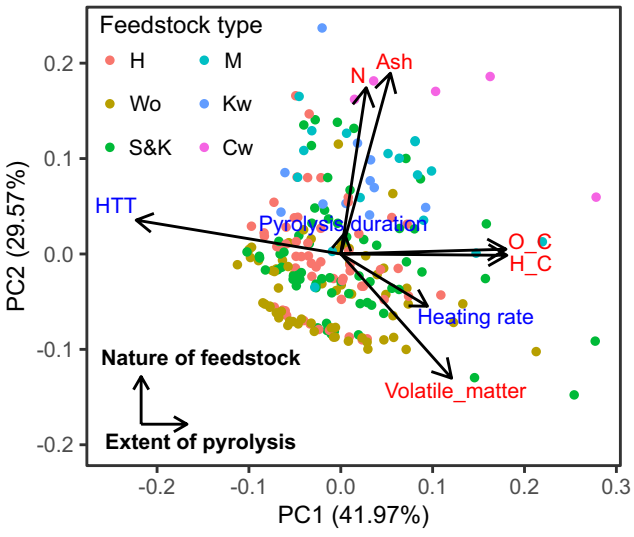

FIGURE 2 Biplot of the first two PCs of PCA. Variables in red are plotted by their scaled loadings on PC1 and PC2, variables in blue are plotted by their scaled coefficient of correlation with PC1 and 2, observations are plotted by their score in the PC space and coloured by feedstock type (H—herbaceous, Wo—woody, S&K—shells and kernels, M—manure, Kw—kitchen waste, NCw—non-cellulosic waste, Cw—cellulosic waste, SS—sewage sludge). The bold black arrows in the lower left-hand corner indicate our interpretation of PC1 and 2.

et al., 2012) biochars. HTT was strongly correlated to PC1 ($r_{Spearman}=0.77$, $p<10^{-15}$). H:C was strongly correlated to HTT ($r_{Spearman}=-0.73$, $p<0.001$, Figure S3 and Table S3). The heating rate was significantly correlated to PC1 with intermediate strength ($r_{Spearman}=0.33$, $p=9.4\times10^{-7}$). Similarly, H:C was significantly and positively correlated to the heating rate ($r_{Spearman}=0.38$, $p<0.001$, Figure S3 and Table S3) despite previous reports of little to no effect of heating rate on ultimate properties of biochar (Chen et al., 2014; Luo et al., 2015). This could be partly explained by the weak correlation between HTT and heating rate ($r_{Spearman}=-0.19$, $p<0.001$). Interestingly, pyrolysis duration was not significantly correlated to PC1 ($r_{Spearman}=0.014$, $p=0.83$). We also did not find a strong correlation between pyrolysis duration and any ultimate or proximate variables (Figure S3 and Table S3, in particular for H:C $r_{Spearman}=-0.09$, $p=8\times10^{-3}$; Crombie & Mašek, 2015; Kearns et al., 2014; Liu et al., 2019). This is in contradiction with previous reports of a decrease in H:C with increasing pyrolysis duration (Ronsse et al., 2013; Suman & Gautam, 2017; Yuan et al., 2013; Zhang et al., 2020) but could be explained by different pyrolysis technology and to some extent by different feedstock particle size (see Section 1) that may blur the effect of this parameter. Exceedingly long pyrolysis durations (e.g. several days) likely weaken the statistical correlation. HTT appears to be the main pyrolysis parameter affecting the extent of pyrolysis.

PC2 was defined by the contribution of ash and N content, with loadings of +0.66 and +0.60 respectively (Table S5), and to a lesser extent VM with a loading of −0.45 (Figure 2). We interpreted PC2 as representing differences between feedstocks, which were separated according to their ash and N content (see also Figure S4). In particular, biochars derived from manure and kitchen waste occupy the upper part of the plot (highest ash and N contents) whereas woody biochars occupy the lower part (lowest ash and N contents). Herbaceous and shells and kernels derived biochars occupy an intermediate position. PC2 was weakly and for the most part not significantly correlated with pyrolysis parameters ($r_{Spearman}=0.12$, 0.19 and 0.07, $p=0.07$, 0.005 and 0.3 for HTT, heating rate and pyrolysis duration respectively). Correlations between all pyrolysis parameters and ash and N contents were very weak (Figure S3 and Table S3).

The intermediate position of VM content, between PC1 and PC2, is consistent with previous reports that VM content is mainly driven by reported HTT (Budai et al., 2014; Campos et al., 2020; Pariyar et al., 2020; Rodriguez Ortiz et al., 2020; Zhang et al., 2017), followed to a lesser extent by pyrolysis duration and feedstock type (Askeland et al., 2019; Cantrell et al., 2012; Khajavi-Shojaei et al., 2020; Mašek et al., 2018; Suman & Gautam, 2017; Yuan et al., 2014). Concerns about the reliability of VM measurement and the partial dependency of VM on feedstock type question the quality of this proxy for the extent of pyrolysis and indicate that HTT is unlikely to be a good predictor of VM.

PCs are orthogonal, which means they are not correlated. Thus, in this restricted data set, the relationship between H:C, O:C and HTT, illustrating the extent of pyrolysis and represented along PC1, was not affected by feedstock type, represented along PC2. Janu et al. (2021) and Zhang et al. (2017) obtained similar PCAs, despite the inclusion of variables characterizing the inorganic content of biochar or derived from FT-IR analysis. In the latter, however, O:C contributes mostly to the feedstock axis. There is unclear evidence on whether or not O:C depends on feedstock type and concerns regarding the reliability of O determination (see previous section). H:C appears to be a more generally applicable indicator of the extent of pyrolysis, as suggested by Budai et al. (2014).

To confirm that all feedstocks show a similar behavior regarding the extent of pyrolysis we calculated the Theil-Sen estimators of the slope and intercept for the log-linear regression of H:C on HTT for each feedstock type (Table 2). The slope of the model is not significantly different from 0 at the 95% bootstrap confidence interval

TABLE 2 Theil-Shen estimators and bootstrap confidence intervals of the slope and intercept for the log-linear regression of H:C on HTT by feedstock type. Values in bold show slopes that are not significantly different from 0 at the 95% bootstrap confidence interval.

		Theil-Sen estimator	Confidence interval	
Feedstock type			**Lower**	**Upper**
Herbaceous	Intercept	1.10	0.91	1.28
	Slope	−0.0037	−0.0041	−0.0033
Woody	Intercept	1.00	0.86	1.15
	Slope	−0.037	−0.0040	−0.0035
Shells and kernels	Intercept	1.06	0.74	1.29
	Slope	−0.0038	−0.0043	−0.0033
Manure	Intercept	0.87	0.41	1.22
	Slope	−0.0035	−0.0042	−0.0029
Kitchen waste	Intercept	1.19	0.33	2.04
	Slope	−0.0035	−0.0042	−0.0029
Non-cellulosic waste	Intercept	1.14	0.68	1.50
	Slope	**−0.0015**	**−0.0038**	**0.0004**
Cellulosic waste	Intercept	1.11	0.68	1.61
	Slope	−0.0034	−0.0046	−0.0025
Sewage sludge	Intercept	1.34	0.67	3.56
	Slope	**−0.0028**	**−0.0062**	**0.0006**

for NC waste and sewage sludge derived biochars. H:C may not be a good indicator of the extent of pyrolysis for feedstocks, which are not mainly made of cellulose, hemicellulose, and lignin and probably form different reaction products. The regression lines for all other feedstocks, for which most of the organic material is lignocellulosic, are overlapping, and their slopes and intercepts are not statistically different from one another at the 95% bootstrap confidence interval (Figure S5 and Table S6). In this large dataset, among cellulosic and lignocellulosic material, there is no effect of feedstock type on the extent of pyrolysis reached under similar HTT. In the remainder of this article, noncellulosic wastes will be excluded from the analysis and herbaceous plants, woody plants, shells and kernels, manure, kitchen waste, and cellulosic waste will be designated as (ligno)cellulosic feedstocks and analyzed together.

3.3 | Evaluation of HTT as a predictor for H:C

Figure 3 shows the regression of H:C on HTT across (ligno) cellulosic feedstocks (model parameters and confidence intervals in Table S7). We used a log-linear mixed model

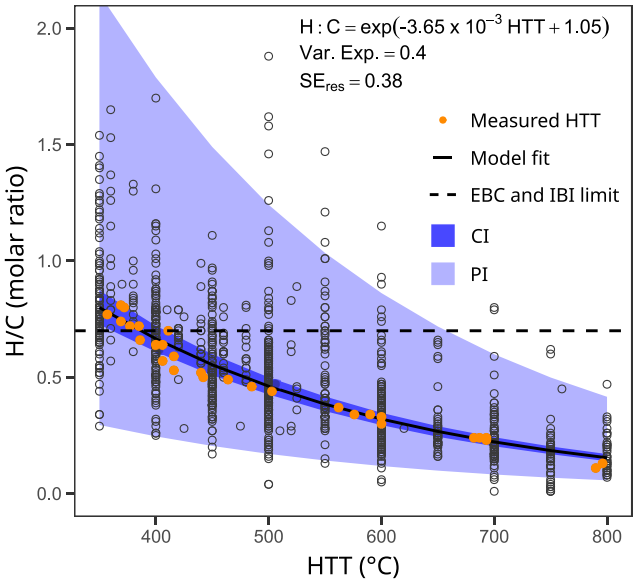

FIGURE 3 Log linear mixed-model regression of H:C versus HTT (solid line) for biochars derived from (ligno)cellulosic feedstocks (black circles) with the confidence (CI, dark blue) and prediction (PI, light blue) bands. The orange dots represent biochar for which HTT was actually measured using thermocouples placed in the pyrolysing biomass (Budai et al., 2014) The IBI (Budai et al., 2013) and EBC (2022) limit H:C ratio for a material to qualify as biochar is overlaid as a dashed line. The equation of the regression line, variance explained by the model and residual standard error are also displayed.

to take into account that data from the same study are likely to be more strongly correlated than data from different studies, for instance because of an oven-dependent systematic bias in HTT or a sample preparation-dependent systematic bias in H:C (see below). This model explains 46% of the variance. The addition of pyrolysis duration as a second predictor variable slightly improved the model (variance explained = 50%, see Figure S6 for 3D visualization and model parameters), but when HTT and pyrolysis duration are scaled to a similar range, the slope coefficient for the latter is one order of magnitude smaller than for the former. The pyrolysis duration effect is of the second order and does not explain by itself the large spread in the data visible in Figure 3. The addition of other predictor variables did not result in a significant improvement of the model. HTT is the single most important explanatory factor of H:C (Askeland et al., 2019; Budai et al., 2014; Crombie et al., 2013; Mukome et al., 2013; Suman & Gautam, 2017; Zhang et al., 2017, 2020). However, we observe an important spread of H:C around the regression line (H:C ranges from 0.61 [Q1] to 0.84 [Q3] for 350°C ≤ HTT < 450°C and from 0.18 [Q1] to 0.33 [Q3] for HTT ≥ 600°C) resulting in a very wide prediction interval. In addition to the effect of pyrolysis duration, this dispersion could arise from biases and errors in the estimation of both variables.

Biochars have a high surface area and tend to take up moisture during cool down and storage. If the samples are not stored appropriately after drying at 105°C or dried immediately before elemental analysis, this water will be released during the analysis and counted as H content of the biochar. For instance, if a sample had taken up to 10 wt% moisture, the error on H:C would be +0.226 for a biochar having 65% C (the median C content in our dataset, see Figure S7 for the dependance of this error on C and moisture contents). This could explain a large part of the observed spread in H:C values, but only in the positive direction. Similarly, hydrated minerals originally present in the feedstock (silica phytoliths in grass for instance) or precipitated during biochar production will likely de-hydrate at the temperature reached during elemental analysis (Balek & Šubrt, 1995; Lippens & de Boer, 1964; Rammelberg et al., 2012). Mineral elements, in particular alkali and alkaline earth, favor the formation of the solid product (biochar) relative to the gaseous and liquid (bio-oil or tar) fractions during pyrolysis (Buss et al., 2019; Eom et al., 2012; Grafmüller et al., 2022; Nowakowski et al., 2007), but the exact mechanisms of char formation, its detailed molecular composition, and the precise effect of mineral elements remains to be elucidated (Anca-Couce, 2016). In particular, the effect on the H:C ratio of the resulting biochar is not systematic: it can change in both directions and tends to be of limited amplitude (Grafmüller et al., 2022; Huang et al., 2017; Raveendran

et al., 1995). Very few studies reported organic carbon content and ratio (C_{org} and $H:C_{org}$) that would allow us to exclude a contribution from inorganic carbon to the measured H:C. Enders et al. (2012) showed that the difference between C and C_{org} is small for biochars derived from woody and herbaceous feedstocks but can be high for poultry manure (see also Wystalska et al., 2021), which contains carbonates, and paper waste. Lange et al. (2018) found high inorganic C content for biochars derived from demolition wood, which could be contaminated with cement, but not for other woody and non-woody feedstocks. The error on H:C due to the failure to account for inorganic C remains below 0.02 units in the positive direction for most biochars except those derived from carbonates contaminated feedstocks (Figure S8). Ash content measured by proximate analysis contains most of these mineral elements. There was no correlation between H:C and ash content overall (Figure S3 and Table S3, $r_{Spearman} = 0.006$, $p = 0.071$), only weak correlations within feedstock types and when ash content was added as a predictive variable to the model both the main effect and interaction term with HTT were not significant at the 95% confidence level. Ash content and composition may play a role in the dispersion of the H:C ratio, to an extent that we are not able to quantify, but do not cause a systematic bias. Finally, concerns have been raised about non-representative sampling of large biochar batches (Bucheli et al., 2014) and only a few authors (Mašek et al., 2018) report sampling methods designed to alleviate this risk.

The dispersion of data could also come from an error in HTT estimation. Most studies in the biochar literature do not report a measured temperature (HTT_{meas}) but the oven set-point (HTT_{set}). HTT_{set} is an approximation of the temperature in a pyrolysing biomass particle. The potential error is related to the location of the temperature measurement in the oven, the difficulty to ensure homogeneous temperature throughout the feedstock bed and biomass particle volume due to heat transfer limitations (1) and thermodynamic effects (2), and the ability of the system to actually control the temperature (3). (1) Temperature measurement used to ensure that HTT_{set} is reached is often done at the surface of the reactor or in the pyrolysis gas stream. The temperature realized in the biomass particle differs from this measurement due to more or less efficient heat transfer from the heating elements to the pyrolysis gas and through the walls of the reactor—Liaw et al. (2012) observed a difference of 170°C between the wall of an Auger reactor and the actual biomass temperature—from the heated gas to the feedstock particles throughout the feedstock bed (Liaw et al., 2012; Mašek et al., 2018; Mesa-Perez et al., 2005) and within larger particles (Park et al., 2010). Taking into account heat transfer limitations is especially important in fast pyrolysis where feedstock is exposed to heat for only a few seconds. Brewer et al. (2012) have shown that the "apparent slow pyrolysis temperatures for these [fast pyrolysis] biochars are [...] well below the actual reactor temperature", with a difference of 75–175°C. (2) Over the most common range of pyrolysis temperatures (400–600°C), volatilization of feedstock moisture and primary pyrolysis reactions (in particular cellulose decomposition) are usually found to be endothermic whereas secondary charring reactions are found to be exothermic (Anca-Couce, 2016). This affects the particle temperature throughout the pyrolysis process (Di Blasi, 1996; Koufopanos et al., 1991; Park et al., 2010; Pyle & Zaror, 1984; Siddiqi et al., 2020; Simmons & Gentry, 1986). Budai et al. (2014) have observed a deviation of 20–120°C between HTT_{meas} and HTT_{set} due to exothermicity in a slow pyrolysis experiment below 400°C. The additional error on H:C that arises from using HTT_{set} instead of measured or re-estimated HTT ranges from 0.14 (min) to 0.48 (max) for fast pyrolysis biochars (data from Brewer et al., 2012) and from −0.15 (min) to 0.07 (max) for slow pyrolysis biochars (data from Budai et al., 2014; Scheme S1 and Table S8). (3) Cantrell and Martins (Cantrell & Martin, 2012) showed that even when measuring the temperature in the centre of the reactor, temperature control in a pyrolysis oven requires advanced methods in control theory. Therefore, the temperature achieved in a pyrolyzing biomass particle, for a given pyrolysis oven technology and configuration, depends on the relative values of the heating rate and residence time in the reactor (time left for the temperature to equilibrate throughout the system and for the reactions to proceed), the amount and size of feedstock particles (volume through which it has to equilibrate), and the feedstock thermo-chemical properties (Antal & Grønli, 2003). Indeed, when attempts were made at properly measuring the temperature in the pyrolyzing feedstock (Budai et al., 2014), the data fell closer to the regression line (orange dots in Figure 3). This discussion is in line with the views presented by Rathnayake et al. (2020) in their introduction. The complexity of pyrolysis temperature control has been discussed since the mid 20th century in the charcoal production literature with the goal of producing relatively homogeneous high-quality char. However, despite recurrent warnings (Cayuela et al., 2022; Rathnayake et al., 2020; Steiner, 2016) and the call for "designer" biochar (selection of production parameters to achieve biochar with properties that correspond to the desired end-use), the biochar community continues to report HTT_{set} in most cases. To achieve complete pyrolysis throughout the feedstock and thus, homogenous biochar quality in a production batch, pyrolysis conditions must be appropriately set, controlled, monitored and reported.

We were not able to estimate of the magnitude of the total uncertainty on H:C and on HTT because some

components of the error lack quantitative estimates in the literature. We cannot unambiguously state which of these variables is responsible for the large dispersion of the data in Figure 3. Nonetheless, any attempt at predicting H:C from HTT would result in potentially large error. Since H:C is a directly measured, chemical characteristic of biochar, whereas HTT_{set} is an approximate and incomplete information on the thermal history of the product, we advise, like others before (Budai et al., 2014; Woolf et al., 2021), that H:C and not reported HTT should be used to predict properties of biochar derived from (ligno) cellulosic feedstocks. H and C measurements were found to be satisfactorily repeatable and reproducible in an inter-laboratory comparison (Bachmann et al., 2016), but representative sampling may be challenging.

3.4 | HTT and H:C as proxies of biochar persistence

Based on 1079 paired observations of HTT and H:C for biochars derived from (ligno)cellulosic feedstocks it is possible to compare estimates of biochar persistence in soil based on both proxies and calculated using Equations (2–4; IPCC, 2019; Woolf et al., 2021). Figure 4 shows the distribution of ΔF_{perm}

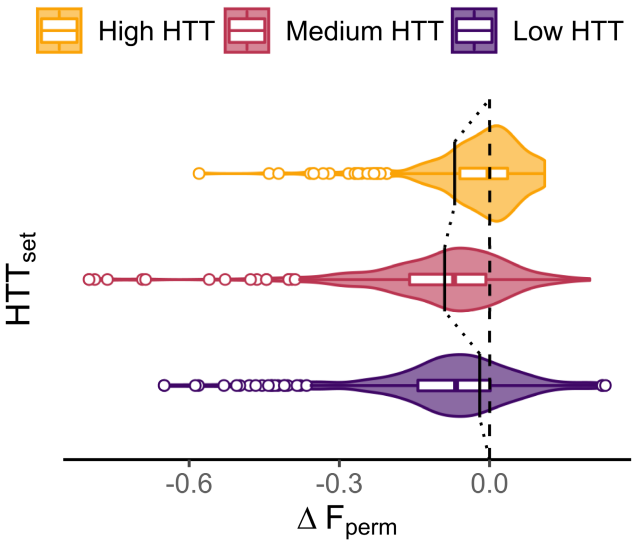

FIGURE 4 Difference between persistence estimate based on H:C and persistence estimate based on HTT according to the IPCC (ΔF_{perm}), for three temperature classes (low for 350°C≤ HTT_{set} < 450°C, medium for 450°C≤ HTT_{set} < 600°C and high for HTT_{set} ≥ 600°C), for biochars derived from (ligno)cellulosic feedstocks. The enveloppe around the boxplots represents the data density. The vertical dashed line at 0 is a guide to visualize the proportion of the data points for which $F_{perm,HTT}$ as per the IPCC (IPCC, 2019) overestimates (negative values) the persistence compared to $F_{perm,H:C}$. The vertical solid lines represent how this proportion shifts when using instead $F_{perm,HTT}$ as per Woolf et al. (2021).

for three temperature classes. Negative values indicate that the persistence is overestimated when using HTT as a predictor relative to H:C. When using Equation (4) to calculate $F_{perm,HTT}$ the persistence is overestimated for 75% of the biochars produced between 350 and 450°C, 80% of the biochars produced between 450 and 600°C and 56% of the biochars produced at or above 600°C. When using Equation (3) instead these proportions are reduced to 70.5%, 45% and 23.5% respectively. This analysis was repeated using five equations for $F_{perm,H:C}$ introduced by Rodrigues et al. (2023) and Azzi et al. (2024) and the results are presented in the online resources (Figure S9 and Table S9). Depending on the selected equation the median bias between $F_{perm,H:C}$ and $F_{perm,HTT}$ varies but Δ Fperm values remain highly dispersed. This is a direct consequence of the spread of H:C for a given HTT_{set} discussed in the previous section. Using HTT as a proxy for biochar persistence in soil, as suggested in the IPCC (2019)'s Guidelines for National Greenhouse Gas Inventories, would result in frequent and sometimes large errors, which could then lead to improper compensation for carbon storage via carbon markets and improper reporting of carbon sinks in local and national carbon accounting schemes.

While pyrolysis temperature has been shown to be the most influential pyrolysis parameter in determining biochar persistence in soil, the difficulty to measure HTT correctly reduces the practical value of the IPCC (2019)'s and Woolf et al. (2021)'s tables of biochar persistence. The lack of agreement between existing equations for $F_{perm,H:C}$ also raises concerns as to the suitability of this proxy. In addition, the estimates of persistence upon which these equations are built are themselves questionable since they are extrapolated from short-term incubation experiments carried out under varying, non-standardized conditions that are not representative of field conditions, and sensitive to data and model selection and fitting procedures (Azzi et al., 2024; Leng et al., 2019). A precise and accurate prediction of biochar persistence in soil and estimation of GHG sequestration from biochar application requires more studies to link robustly estimated biochar persistence to biochar characteristics correctly measured using standardized protocols. It also calls for an effort of the biochar scientific community to monitor and report precisely and accurately measured pyrolysis parameters and to develop standard methods to assess carbon stability and related proxies with higher precision and repeatability.

4 | CONCLUSION

In this study, we collected and made available a large dataset of biochar production conditions and physicochemical characteristics. We confirm that, for biochars

derived from (ligno)cellulosic feedstocks, characteristics (H:C, O:C, N, ash, and VM content) can be *explained* by pyrolysis parameters (feedstock type, extent of pyrolysis), but we show that the usual proxies of biochar persistence in soil (H:C, O:C, VM) cannot be *accurately predicted* from HTT because of a lack of quality in the dataset present in the literature and major difficulties in correctly measuring the pyrolysis temperature. By extension, the prediction of biochar persistence in soil from HTT is subject to large uncertainties, which reduces the practical value of tabulated biochar persistence estimates based on this parameter.

To achieve complete pyrolysis throughout the feedstock and, thus, homogenous biochar quality of a production batch, pyrolysis conditions must be monitored appropriately. In particular, pyrolysis temperature should be measured at appropriate spots within the feedstock or advanced models including heat transfer rate, particle size, and the energy balance of pyrolysis reactions under the given pyrolysis conditions in the reactor should be used. Otherwise, we advise that actual biochar characteristics are measured via ultimate and proximate analysis, keeping in mind that representative sampling and analysis may be challenging especially when using small sample sizes.

To conclude, we stress the importance of (1) complying with standardized analytical methods for biochar, (2) monitoring and understanding the influence of pyrolysis conditions on biochar characteristics, and (3) developing new standard methods to assess biochar carbon persistence in soils and related proxies with higher precision and repeatability. We recommend that the calculation of biochar C persistence presented in the IPCC (2019)'s Guidelines for National Greenhouse Gas Inventories is rapidly improved.

SUPPLEMENTARY INFORMATION

Summary and test statistics, and regression model outputs broken down per feedstock type; diagnostic plot for the PCA; pairwise correlation between production parameters and physico-chemical characteristics; quantitative estimates of the error on H:C including effect of moisture, inorganic C and additional error due to HTT; and extended results and discussion regarding ΔF_{perm} are provided in Supplementary information.

AUTHOR CONTRIBUTIONS

Johanne Lebrun Thauront: Data curation; formal analysis; investigation; visualization; writing – original draft; writing – review and editing. **Gerhard Soja:** Investigation; writing – review and editing. **Hans-Peter Schmidt:** Conceptualization; writing – review and editing. **Samuel Abiven:** Conceptualization; funding acquisition; supervision; writing – review and editing.

ACKNOWLEDGMENTS

JLT and SA thank the Centre National de la Recherche Scientifique (CNRS) for funding the MITI *CPyPaysage* project. All authors thank the three anonymous reviewers for their detailed and constructive feedback.

FUNDING INFORMATION

Financial support for this research was received from CNRS (MITI *CPyPaysage* project).

CONFLICT OF INTEREST STATEMENT

The authors have no relevant financial or non-financial interests to disclose.

DATA AVAILABILITY STATEMENT

The data that support the findings of this study are openly available in Zenodo at https://doi.org/10.5281/zenodo.10394581 (Lebrun Thauront et al., 2024).

ORCID

Johanne Lebrun Thauront https://orcid.org/0000-0002-7248-0723
Gerhard Soja https://orcid.org/0000-0001-7391-4899
Hans-Peter Schmidt https://orcid.org/0000-0001-8275-7506
Samuel Abiven https://orcid.org/0000-0002-5663-0912

REFERENCES

Abiven, S., Schmidt, M. W., & Lehmann, J. (2014). Biochar by design. *Nature Geoscience*, *7*(5), 326–327. https://doi.org/10.1038/ngeo2154

Amin, F. R., Huang, Y., He, Y., Zhang, R., Liu, G., & Chen, C. (2016). Biochar applications and modern techniques for characterization. *Clean Technologies and Environmental Policy*, *18*(5), 1457–1473. https://doi.org/10.1007/s10098-016-1218-8

Anca-Couce, A. (2016). Reaction mechanisms and multi-scale modelling of lignocellulosic biomass pyrolysis. *Progress in Energy and Combustion Science*, *53*(2016), 41–79. https://doi.org/10.1016/j.pecs.2015.10.002

Antal, M. J., & Grønli, M. (2003). The art, science, and technology of charcoal production. *Industrial and Engineering Chemistry Research*, *42*(8), 1619–1640. https://doi.org/10.1021/ie0207919

Askeland, M., Clarke, B., & Paz-Ferreiro, J. (2019). Comparative characterization of biochars produced at three selected pyrolysis temperatures from common woody and herbaceous waste streams. *PeerJ*, *7*, 1–20. https://doi.org/10.7717/peerj.6784

Azzi, E. S., Li, H., Cederlund, H., Karltun, E., & Sundberg, C. (2024). Modelling biochar long-term carbon storage in soil with harmonized analysis of decomposition data. *Geoderma*, *441*(October), 116761. https://doi.org/10.1016/j.geoderma.2023.116761

Bachmann, H. J., Bucheli, T. D., Dieguez-Alonso, A., Fabbri, D., Knicker, H., Schmidt, H. P., Ulbricht, A., Becker, R., Buscaroli, A., Buerge, D., Cross, A., Dickinson, D., Enders, A., Esteves, V. I., Evangelou, M. W. H., Fellet, G., Friedrich, K., Gasco Guerrero, G., Glaser, B., ... Zehetner, F. (2016). Toward the standardization of biochar analysis: The COST action TD1107 Interlaboratory comparison. *Journal of Agricultural and Food Chemistry*, *64*(2), 513–527. https://doi.org/10.1021/acs.jafc.5b05055

Balek, V., & Šubrt, J. (1995). Thermal behaviour of iron(lll) oxide hydroxides. *Pure and Applied Chemistry*, *67*(11), 1839–1842. https://doi.org/10.1351/pac199567111839

Bates, D., Maechler, M., Bolker, B., & Walker, S. (2015). Linear mixed-effects models using 'Eigen' and S4. *Journal of Statistical Software*, *67*(1), 1–48. https://doi.org/10.18637/jss.v067.i01

Bowring, S. P., Jones, M. W., Ciais, P., Guenet, B., & Abiven, S. (2022). Pyrogenic carbon decomposition critical to resolving fire's role in the earth system. *Nature Geoscience*, *15*(2), 135–142. https://doi.org/10.1038/s41561-021-00892-0

Brewer, C. E., Chuang, V. J., Masiello, C. A., Gonnermann, H., Gao, X., Dugan, B., Driver, L. E., Panzacchi, P., Zygourakis, K., & Davies, C. A. (2014). New approaches to measuring biochar density and porosity. *Biomass and Bioenergy*, *66*, 176–185. https://doi.org/10.1016/j.biombioe.2014.03.059

Brewer, C. E., Hu, Y.-Y., Schmidt-Rohr, K., Loynachan, T. E., Laird, D. A., & Brown, R. C. (2012). Extent of pyrolysis impacts on fast pyrolysis biochar properties. *Journal of Environmental Quality*, *41*(4), 1115–1122. https://doi.org/10.2134/jeq2011.0118

Brewer, C. E., Schmidt-Rohr, K., Satrio, J. A., & Brown, R. C. (2009). Characterization of biochar from fast pyrolysis and gasification systems. *Environmental Progress & Sustainable Energy*, *28*(3), 386–396.

Bucheli, T. D., Bachmann, H. J., Blum, F., Bürge, D., Giger, R., Hilber, I., Keita, J., Leifeld, J., & Schmidt, H. P. (2014). On the heterogeneity of biochar and consequences for its representative sampling. *Journal of Analytical and Applied Pyrolysis*, *107*, 25–30. https://doi.org/10.1016/j.jaap.2014.01.020

Budai, A., Wang, L., Gronli, M., Strand, L. T., Antal, M. J., Abiven, S., Dieguez-Alonso, A., Anca-Couce, A., & Rasse, D. P. (2014). Surface properties and chemical composition of corncob and miscanthus biochars: Effects of production temperature and method. *Journal of Agricultural and Food Chemistry*, *62*(17), 3791–3799. https://doi.org/10.1021/jf501139f

Budai, A., Zimmerman, A. R., Cowie, A. L., Webber, J. B. W., Singh, B. P., Glaser, B., Masiello, C. A., Andersson, D., Shields, F., Lehmann, J., Arbestain, M. C., Williams, M., Sohi, S., & Joseph, S. (2013). Biochar carbon stability test method: An assessment of methods to determine biochar carbon stability. *International Biochar Initiative*, 1–10.

Buss, W., Jansson, S., & Mašek, O. (2019). Unexplored potential of novel biochar-ash composites for use as organomineral fertilizers. *Journal of Cleaner Production*, *208*, 960–967. https://doi.org/10.1016/j.jclepro.2018.10.189

Campos, P., Miller, A. Z., Knicker, H., Costa-Pereira, M. F., Merino, A., & De la Rosa, J. M. (2020). Chemical, physical and morphological properties of biochars produced from agricultural residues: Implications for their use as soil amendment. *Waste Management*, *105*, 256–267. doi:10.1016/j.wasman.2020.02.013

Camps Arbestain, M., Amonette, J. E., Singh, B., Wang, T., & Schmidt, H. P. (2015). A biochar classification system and associated test methods. In J. Lehmann & S. Joseph (Eds.), *Biochar for environmental management—Science and technology* (2nd ed., p. 928). Routledge.

Cantrell, K. B., Hunt, P. G., Uchimiya, M., Novak, J. M., & Ro, K. S. (2012). Impact of pyrolysis temperature and manure source on physicochemical characteristics of biochar. *Bioresource Technology*, *107*, 419–428. https://doi.org/10.1016/j.biortech.2011.11.084

Cantrell, K. B., & Martin, J. H. (2012). Stochastic state-space temperature regulation of biochar production. Part I: Theoretical development. *Journal of the Science of Food and Agriculture*, *92*(3), 481–489. https://doi.org/10.1002/jsfa.4618

Canty, A., & Ripley, B. D. (2022). *Boot: Bootstrap R (S-plus) functions*.

Cayuela, M. L., Cowie, A., & Laird, D. (2022). Top tips to avoid desk rejection—How to avoid desk-rejection: Biochar studies. https://www.sciencedirect.com/journal/geoderma/about/top-tips-to-avoid-desk-rejection

Cheah, S., Malone, S. C., & Feik, C. J. (2014). Speciation of sulfur in biochar produced from pyrolysis and gasification of oak and corn stover. *Environmental Science and Technology*, *48*(15), 8474–8480. https://doi.org/10.1021/es500073r

Chen, D., Zhou, J., & Zhang, Q. (2014). Effects of heating rate on slow pyrolysis behavior, kinetic parameters and products properties of moso bamboo. *Bioresource Technology*, *169*, 313–319. https://doi.org/10.1016/j.biortech.2014.07.009

Chun, Y., Sheng, G., Chiou, G. T., & Xing, B. (2004). Compositions and sorptive properties of crop residue-derived chars. *Environmental Science and Technology*, *38*(17), 4649–4655. https://doi.org/10.1021/es035034w

Crane-Droesch, A., Abiven, S., Jeffery, S., & Torn, M. S. (2013). Heterogeneous global crop yield response to biochar: A meta-regression analysis. *Environmental Research Letters*, *8*(4), 1–8. https://doi.org/10.1088/1748-9326/8/4/044049

Crombie, K., & Mašek, O. (2015). Pyrolysis biochar systems, balance between bioenergy and carbon sequestration. *GCB Bioenergy*, *7*(2), 349–361. https://doi.org/10.1111/gcbb.12137

Crombie, K., Mašek, O., Sohi, S. P., Brownsort, P., & Cross, A. (2013). The effect of pyrolysis conditions on biochar stability as determined by three methods. *GCB Bioenergy*, *5*(2), 122–131. https://doi.org/10.1111/gcbb.12030

Davinson, A. C., & Hinkley, D. V. (1997). *Bootstrap methods and their applications*. Cambridge University Press. http://statwww.epfl.ch/davison/BMA/

de la Rosa, J. M., Paneque, M., Miller, A. Z., & Knicker, H. (2014). Relating physical and chemical properties of four different biochars and their application rate to biomass production of Lolium perenne on a calcic Cambisol during a pot experiment of 79 days. *Science of the Total Environment*, *499*, 175–184. https://doi.org/10.1016/j.scitotenv.2014.08.025

Di Blasi, C. (1996). Kinetic and heat transfer control in the slow and flash pyrolysis of solids. *Industrial and Engineering Chemistry Research*, *35*(1), 37–46. https://doi.org/10.1021/ie950243d

EBC. (2022). European Biochar Certificate—Guidelines for a sustainable production of biochar, Frick, Switzerland. http://european-biochar.org

Enders, A., Hanley, K., Whitman, T., Joseph, S., & Lehmann, J. (2012). Characterization of biochars to evaluate recalcitrance and agronomic performance. *Bioresource Technology*, *114*, 644–653. Retrieved from. https://doi.org/10.1016/j.biortech.2012.03.022

Eom, I. Y., Kim, J. Y., Kim, T. S., Lee, S. M., Choi, D., Choi, I. G., & Choi, J. W. (2012). Effect of essential inorganic metals on primary thermal degradation of lignocellulosic biomass. *Bioresource Technology*, *104*, 687–694. https://doi.org/10.1016/j.biortech.2011.10.035

Fan, J., Li, Y., Yu, H., Li, Y., Yuan, Q., Xiao, H., Li, F., & Pan, B. (2020). Using sewage sludge with high ash content for biochar production and Cu(II) sorption. *Science of the Total Environment*, *713*, 136663. https://doi.org/10.1016/j.scitotenv.2020.136663

Fang, Y., Singh, B., Singh, B. P., & Krull, E. (2014). Biochar carbon stability in four contrasting soils. *European Journal of Soil Science*, *65*(1), 60–71. https://doi.org/10.1111/ejss.12094

Fang, Y., Singh, B. P., Nazaries, L., Keith, A., Tavakkoli, E., Wilson, N., & Singh, B. (2019). Interactive carbon priming, microbial response and biochar persistence in a vertisol with varied inputs of biochar and labile organic matter. *European Journal of Soil Science*, *70*(5), 960–974. https://doi.org/10.1111/ejss.12808

Gaunt, J., & Cowie, A. (2009). Biochar, greenhouse gas accounting and emissions trading. In J. Lehmann & S. Joseph (Eds.), *Biochar for environmental management—Science and technology* (1st ed., p. 405). Earthscan.

Grafmüller, J., Böhm, A., Zhuang, Y., Spahr, S., Müller, P., Otto, T. N., & Hagemann, N. (2022). Wood ash as an additive in biomass pyrolysis: Effects on biochar yield, properties, and agricultural performance. *ACS Sustainable Chemistry and Engineering*, *10*(8), 2720–2729. https://doi.org/10.1021/acssuschemeng.1c07694

Haman, J., & Avery, M. (2020). ciTools: Confidence or prediction intervals, quantiles, and Probabilitiesfor statistical models. https://cran.r-project.org/package=ciTools

Harrell, F. E. J. (2023). Hmisc: Harrell Miscellaneous. https://hbiostat.org/R/Hmisc/, https://cran.r-project.org/package=Hmisc

Harvey, O. R., Herbert, B. E., Rhue, R. D., & Kuo, L. J. (2011). Metal interactions at the biochar-water interface: Energetics and structure-sorption relationships elucidated by flow adsorption microcalorimetry. *Environmental Science and Technology*, *45*(13), 5550–5556. https://doi.org/10.1021/es104401h

Hassan, M., Liu, Y., Naidu, R., Parikh, S. J., Du, J., Qi, F., & Willett, I. R. (2020). Influences of feedstock sources and pyrolysis temperature on the properties of biochar and functionality as adsorbents: A meta-analysis. *Science of the Total Environment*, *744*, 1–15. https://doi.org/10.1016/j.scitotenv.2020.140714

Horikoshi, M., Tang, Y., Dickey, A., Grenié, M., Thompson, R., Selzer, L., Strbenac, D., Voronin, K., & Pulatov, D. (2018). *Ggfortify: Data visualization tools for statistical analysis results*. https://github.com/sinhrks/ggfortify, https://cran.r-project.org/package=ggfortify

Huang, H.-J., Yang, T., Ying Lai, F., & Qiang Wu, G. (2017). Co-pyrolysis of sewage sludge and sawdust/rice straw for the production of biochar. *Journal of Analytical and Applied Pyrolysis*, *125*(March), 61–68. https://doi.org/10.1016/j.jaap.2017.04.018

IPCC. (2019). Method for estimating the change in mineral soil organic carbon stocks from biochar amendments: Basis for future methodological development. 2019 refinement to the 2006 IPCC Guidelines for National Greenhouse Gas Inventories, Ap4.1 https://www.ipcc-nggip.iges.or.jp/public/2019rf/pdf/4_Volume4/19R_V4_Ch02_Ap4_Biochar.pdf

IPCC. (2023). In H. Lee & J. Romero (Eds.), *Climate change 2023: Synthesis report (Core Writing Team)*. Author. https://www.unep.org/resources/report/climate-change-2023-synthesis-report

Ippolito, J. A., Cui, L., Kammann, C., Wrage-Mönnig, N., Estavillo, J. M., Fuertes-Mendizabal, T., Cayuela, M. L., Sigua, G., Novak, J., Spokas, K., & Borchard, N. (2020). Feedstock choice, pyrolysis temperature and type influence biochar characteristics: A comprehensive meta-data analysis review. *Biochar*, *2*(4), 421–438. https://doi.org/10.1007/s42773-020-00067-x

Janu, R., Mrlik, V., Ribitsch, D., Hofman, J., Sedláček, P., Bielská, L., & Soja, G. (2021). Biochar surface functional groups as affected by biomass feedstock, biochar composition and pyrolysis temperature. *Carbon Resources Conversion*, *4*(November), 36–46. https://doi.org/10.1016/j.crcon.2021.01.003

Kearns, J. P., Wellborn, L. S., Summers, R. S., & Knappe, D. R. (2014). 2,4-D adsorption to biochars: Effect of preparation conditions on equilibrium adsorption capacity and comparison with commercial activated carbon literature data. *Water Research*, *62*, 20–28. https://doi.org/10.1016/j.watres.2014.05.023

Keiluweit, M., Nico, P. S., Johnson, M., & Kleber, M. (2010). Dynamic molecular structure of plant biomass-derived black carbon (biochar). *Environmental Science and Technology*, *44*(4), 1247–1253. https://doi.org/10.1021/es9031419

Khajavi-Shojaei, S., Moezzi, A., Norouzi Masir, M., & Taghavi, M. (2020). Characteristics of conocarpus wastes and common reed biochars as a predictor of potential environmental and agronomic applications. Energy Sources, Part A: Recovery, Utilization and Environmental Effects https://doi.org/10.1080/15567036.2020.1783396

Kim, K. H., Kim, J. Y., Cho, T. S., & Choi, J. W. (2012). Influence of pyrolysis temperature on physicochemical properties of biochar obtained from the fast pyrolysis of pitch pine (Pinus rigida). *Bioresource Technology*, *118*, 158–162. https://doi.org/10.1016/j.biortech.2012.04.094

Koufopanos, C. A., Papayannakos, N., Maschio, G., & Lucchesi, A. (1991). Studies on kinetics, thermal and heat transfer effects. *The Canadian Journal of Chemical Engineering*, *69*, 907–915.

Lange, S. F., Allaire, S. E., Charles, A., Auclair, I. K., & Bajzak, C. E. (2018). *Physicochemical properties of 43 biochars*. Université Laval and GECA Environment. https://doi.org/10.13140/RG.2.2.25450.41924

Lebrun Thauront, J., Soja, G., Schmidt, H. P., & Abiven, S. (2024). Biochar production parameters and physicochemical characteristicse. [Dataset] Zenodo https://doi.org/10.5281/zenodo.10394580

Lee, J. W., Kidder, M., Evans, B. R., Paik, S., Buchanan, A. C., Garten, C. T., & Brown, R. C. (2010). Characterization of biochars produced from cornstovers for soil amendment. *Environmental Science and Technology*, *44*(20), 7970–7974. https://doi.org/10.1021/es101337x

Lehmann, J., & Joseph, S. (Eds.). (2009). *Biochar for environmental management, science and technology* (1st ed.). Earthscan.

Leng, L., Xu, X., Wei, L., Fan, L., Huang, H., Li, J., Lu, Q., Li, J., & Zhou, W. (2019). Biochar stability assessment by incubation and modelling: Methods, drawbacks and recommendations. *Science of the Total Environment*, *664*, 11–23. https://doi.org/10.1016/j.scitotenv.2019.01.298

Leng, L., Yang, L., Lei, X., Zhang, W., Ai, Z., Yang, Z., Zhan, H., Yang, J., Yuan, X., Peng, H., & Li, H. (2022). Machine learning predicting and engineering the yield, N content, and specific surface area of biochar derived from pyrolysis of biomass. *Biochar*, *4*(1), 63–81. https://doi.org/10.1007/s42773-022-00183-w

Liaw, S. S., Wang, Z., Ndegwa, P., Frear, C., Ha, S., Li, C. Z., & Garcia-Perez, M. (2012). Effect of pyrolysis temperature on the yield and properties of bio-oils obtained from the auger pyrolysis of Douglas fir wood. *Journal of Analytical and Applied Pyrolysis*, *93*, 52–62. https://doi.org/10.1016/j.jaap.2011.09.011

Lippens, B. C., & de Boer, J. H. (1964). Study of phase transformations during calcination of aluminum hydroxides by selected area electron diffraction. *Acta Crystallographica*, *17*(10), 1312–1321. https://doi.org/10.1107/s0365110x64003267

Liu, B., Liu, Q., Wang, X., Bei, Q., Zhang, Y., Lin, Z., Liu, G., Zhu, J., Hu, T., Jin, H., Wang, H., Sun, X., Lin, X., & Xie, Z. (2020). A fast chemical oxidation method for predicting the long-term mineralization of biochar in soils. *Science of the Total Environment*, *718*, 137390. https://doi.org/10.1016/j.scitotenv.2020.137390

Liu, Z., Lu, B., He, B., Li, X., & Wang, L. (2019). Effect of the pyrolysis duration and the addition of zeolite powder on the leaching toxicity of copper and cadmium in biochar produced from four different aquatic plants. *Ecotoxicology and Environmental Safety*, *183*(August), 109517. doi:10.1016/j.ecoenv.2019.109517

Luo, L., Xu, C., Chen, Z., & Zhang, S. (2015). Properties of biomass-derived biochars: Combined effects of operating conditions and biomass types. *Bioresource Technology*, *192*, 83–89. https://doi.org/10.1016/j.biortech.2015.05.054

Mašek, O., Buss, W., Roy-Poirier, A., Lowe, W., Peters, C., Brownsort, P., Mignard, D., Pritchard, C., & Sohi, S. (2018). Consistency of biochar properties over time and production scales: A characterisation of standard materials. *Journal of Analytical and Applied Pyrolysis*, *132*(February), 200–210. https://doi.org/10.1016/j.jaap.2018.02.020

Mesa-Perez, J. M., Cortez, L. A., Rocha, J. D., Brossard-Perez, L. E., & Olivares-Gómez, E. (2005). Unidimensional heat transfer analysis of elephant grass and sugar cane bagasse slow pyrolysis in a fixed bed reactor. *Fuel Processing Technology*, *86*(5), 565–575. https://doi.org/10.1016/j.fuproc.2004.05.014

Moses, T., & Klockars, A. (2009). *Strategies for testing slope differences (October)*. Educational Testing Services (ETS).

Moško, J., Pohořelý, M., Skoblia, S., Fajgar, R., Straka, P., Soukup, K., Beňo, Z., Farták, J., Bičáková, O., Jeremiáš, M., Šyc, M., & Meers, E. (2021). Structural and chemical changes of sludge derived pyrolysis char prepared under different process temperatures. *Journal of Analytical and Applied Pyrolysis*, *156*, 105085. https://doi.org/10.1016/j.jaap.2021.105085

Mukome, F. N., Zhang, X., Silva, L. C., Six, J., & Parikh, S. J. (2013). Use of chemical and physical characteristics to investigate trends in biochar feedstocks. *Journal of Agricultural and Food Chemistry*, *61*(9), 2196–2204. https://doi.org/10.1021/jf3049142

Novak, J., Lima, I., Xing, B., Gaskin, J., Steiner, C., Das, K., & Busscher, W. (2009). Characterization of designer biochar produced at different temperatures and their effects on a loamy sand. *Annals of Environmental Science*, *3*(1), 195–206.

Nowakowski, D. J., Jones, J. M., Brydson, R. M., & Ross, A. B. (2007). Potassium catalysis in the pyrolysis behaviour of short rotation willow coppice. *Fuel*, *86*(15), 2389–2402. https://doi.org/10.1016/j.fuel.2007.01.026

Palansooriya, K. N., Li, J., Dissanayake, P. D., Suvarna, M., Li, L., Yuan, X., Sarkar, B., Tsang, D. C. W., Rinklebe, J., Wang, X., & Ok, Y. S. (2022). Prediction of soil heavy metal immobilization by biochar using machine learning. *Environmental Science and Technology*, *56*(7), 4187–4198. https://doi.org/10.1021/acs.est.1c08302

Pariyar, P., Kumari, K., Jain, M. K., & Jadhao, P. S. (2020). Evaluation of change in biochar properties derived from different feedstock and pyrolysis temperature for environmental and agricultural application. *Science of the Total Environment*, *713*, 136433. https://doi.org/10.1016/j.scitotenv.2019.136433

Park, W. C., Atreya, A., & Baum, H. R. (2010). Experimental and theoretical investigation of heat and mass transfer processes during wood pyrolysis. *Combustion and Flame*, *157*(3), 481–494. https://doi.org/10.1016/j.combustflame.2009.10.006

Pyle, D. L., & Zaror, C. A. (1984). Heat transfer and kinetics in the low temperature pyrolysis of solids. *Chemical Engineering Science*, *39*(1), 147–158.

Qiu, M., Sun, K., Jin, J., Han, L., Sun, H., Zhao, Y., Xia, X., Wu, F., & Xing, B. (2015). Metal/metalloid elements and polycyclic aromatic hydrocarbon in various biochars: The effect of feedstock, temperature, minerals, and properties. *Environmental Pollution*, *206*, 298–305. https://doi.org/10.1016/j.envpol.2015.07.026

R Core Team. (2021). *R: A language and environment for statistical computing*. R Foundation for Statistical Computing. https://www.r-project.org

Rammelberg, H. U., Schmidt, T., & Ruck, W. (2012). Hydration and dehydration of salt hydrates and hydroxides for thermal energy storage—Kinetics and energy release. *Energy Procedia*, *30*, 362–369. https://doi.org/10.1016/j.egypro.2012.11.043

Rathnayake, D., Maziarka, P., Ghysels, S., Mašek, O., Sohi, S., & Ronsse, F. (2020). How to trace back an unknown production temperature of biochar from chemical characterization methods in a feedstock independent way. *Journal of Analytical and Applied Pyrolysis*, *151*(August), 104926. https://doi.org/10.1016/j.jaap.2020.104926

Raveendran, K., Ganesh, A., & Khilar, K. C. (1995). Influence of mineral matter on biomass pyrolysis characteristics. *Fuel*, *74*(12), 1812–1822. https://doi.org/10.1016/0016-2361(95)80013-8

Rodrigues, L., Budai, A., Elsgaard, L., Hardy, B., Keel, S. G., Mondini, C., Plaza, C., & Leifeld, J. (2023). The importance of biochar quality and pyrolysis yield for soil carbon sequestration in practice. *European Journal of Soil Science*, *74*(4), 1–11. https://doi.org/10.1111/ejss.13396

Rodriguez Ortiz, L., Torres, E., Zalazar, D., Zhang, H., Rodriguez, R., & Mazza, G. (2020). Influence of pyrolysis temperature and bio-waste composition on biochar characteristics. *Renewable Energy*, *155*, 837–847. https://doi.org/10.1016/j.renene.2020.03.181

Ronsse, F., van Hecke, S., Dickinson, D., & Prins, W. (2013). Production and characterization of slow pyrolysis biochar: Influence of feedstock type and pyrolysis conditions. *GCB Bioenergy*, *5*(2), 104–115. https://doi.org/10.1111/gcbb.12018

Posit team. (2021). RStudio: Integrated Development Environment for R. Posit Software, PBC, Boston, MA. http://www.posit.co/

Schmidt, H. P., Kammann, C., Hagemann, N., Leifeld, J., Bucheli, T. D., Sánchez Monedero, M. A., & Cayuela, M. L. (2021). Biochar in agriculture—A systematic review of 26 global meta-analyses. *GCB Bioenergy*, *13*(11), 1708–1730. https://doi.org/10.1111/gcbb.12889

Siddiqi, H., Kumari, U., Biswas, S., Mishra, A., & Meikap, B. C. (2020). A synergistic study of reaction kinetics and heat transfer with multi-component modelling approach for the pyrolysis of biomass waste. *Energy*, *204*, 117933. https://doi.org/10.1016/j.energy.2020.117933

Simmons, G. M., & Gentry, M. (1986). Particle size limitations due to heat transfer in determining pyrolysis kinetics of biomass. *Journal of Analytical and Applied Pyrolysis*, *10*(2), 117–127. https://doi.org/10.1016/0165-2370(86)85011-2

Singh, B. P., Cowie, A. L., & Smernik, R. J. (2012). Biochar carbon stability in a clayey soil as a function of feedstock and pyrolysis temperature. *Environmental Science and Technology*, *46*(21), 11770–11778. https://doi.org/10.1021/es302545b

Singh, N., Abiven, S., Torn, M. S., & Schmidt, M. W. (2012). Fire-derived organic carbon in soil turns over on a centennial scale. *Biogeosciences*, *9*(8), 2847–2857.

Sohi, S. P., McDonagh, J., Novak, J. M., Wu, W., & Miu, L.-M. (2015). Biochar systems and system fit. In J. Lehmann & S. Joseph (Eds.), *Biochar for environmental management—Science and technology* (2nd ed., p. 928). Routledge.

Spokas, K. A. (2010). Review of the stability of biochar in soils: Predictability of O:C molar ratios. *Carbon Management*, *1*(2), 289–303. https://doi.org/10.4155/cmt.10.32

Steiner, C. (2016). Considerations in biochar characterization. In M. Guo, Z. He, & S. M. Uchimiya (Eds.), *Agricultural and environmental applications of biochar: Advances and barriers (chap. 5)*. Soil Science Society of America.

Suman, S., & Gautam, S. (2017). Effect of pyrolysis time and temperature on the characterization of biochars derived from biomass. *Energy Sources, Part A: Recovery, Utilization and Environmental Effects*, *39*(9), 933–940. https://doi.org/10.1080/15567036.2016.1276650

Sun, K., Kang, M., Zhang, Z., Jin, J., Wang, Z., Pan, Z., Xu, D., Wu, F., & Xing, B. (2013). Impact of deashing treatment on biochar structural properties and potential sorption mechanisms of phenanthrene. *Environmental Science and Technology*, *47*(20), 11473–11481. https://doi.org/10.1021/es4026744

Tang, Y., Horikoshi, M., & Li, W. (2016). Ggfortify: Unified interface to visualize statistical result of popular R packages. *The R Journal*, *8*(2), 478–489. https://doi.org/10.32614/RJ-2016-060

Tintner, J., Preimesberger, C., Pfeifer, C., Theiner, J., Ottner, F., Wriessnig, K., Puchberger, M., & Smidt, E. (2020). Pyrolysis profile of a rectangular kiln—Natural scientific investigation of a traditional charcoal production process. *Journal of Analytical and Applied Pyrolysis*, *146*(December), 104757.

Uchimiya, M., Wartelle, L. H., Klasson, K. T., Fortier, C. A., & Lima, I. M. (2011). Influence of pyrolysis temperature on biochar property and function as a heavy metal sorbent in soil. *Journal of Agricultural and Food Chemistry*, *59*(6), 2501–2510. https://doi.org/10.1021/jf104206c

Venables, W. N., & Ripley, B. D. (2002). *Modern applied statistics with S* (4th ed.). Springer. https://www.stats.ox.ac.uk/pub/MASS4/

Wei, L., Huang, Y., Li, Y., Huang, L., Mar, N. N., Huang, Q., & Liu, Z. (2017). Biochar characteristics produced from rice husks and their sorption properties for the acetanilide herbicide metolachlor. *Environmental Science and Pollution Research*, *24*(5), 4552–4561. https://doi.org/10.1007/s11356-016-8192-x

Wei, T., & Simko, V. (2021). R package "corrplot": Vizualization of a correlation matrix. https://github.com/taiyun/corrplot

Wickham, H., Averick, M., Bryan, J., Chang, W., McGowan, L., François, R., Grolemund, G., Hayes, A., Henry, L., Hester, J., Kuhn, M., Pedersen, T., Miller, E., Bache, S., Müller, K., Ooms, J., Robinson, D., Seidel, D., Spinu, V., … Yutani, H. (2019). Welcome to the tidyverse. *Journal of Open Source Software*, *4*(43), 1686. https://doi.org/10.21105/joss.01686

Wiedemeier, D. B., Abiven, S., Hockaday, W. C., Keiluweit, M., Kleber, M., Masiello, C. A., McBeath, A. V., Nico, P. S., Pyle, L. A., Schneider, M. P. W., Smernik, R. J., Wiesenberg, G. L. B., & Schmidt, M. W. I. (2015). Aromaticity and degree of aromatic condensation of char. *Organic Geochemistry*, *78*, 135–143. https://doi.org/10.1016/j.orggeochem.2014.10.002

Wilcox, R. R. (1998). A note on the Theil-Sen regression estimator when the Regressor is random and the error term is heteroscedastic. *Biometrical Journal*, *40*(3), 261–268.

Wilcox, R. R., & Clark, F. (2013). Robust regression estimators when there are tied values. *Journal of Modern Applied Statistical Methods*, *12*(2), 20–34. https://doi.org/10.22237/jmasm/1383278520

Wilcox, R. R., & Schönbrodt, F. D. (2014). The WRS package for robust statistics in R. http://r-forge.r-project.org/projects/wrs/

Wilke, C. O. (2020). cowplot—Streamlined plot theme and plot annotations for 'ggplot2'. https://wilkelab.org/cowplot/

Woolf, D., Lehmann, J., Ogle, S., Kishimoto-Mo, A. W., McConkey, B., & Baldock, J. (2021). Greenhouse gas inventory model for biochar additions to soil. *Environmental Science & Technology*, *55*, 14795–14805. https://doi.org/10.1021/acs.est.1c02425

Wurster, C. M., Saiz, G., Schneider, M. P., Schmidt, M. W., & Bird, M. I. (2013). Quantifying pyrogenic carbon from thermosequences of wood and grass using hydrogen pyrolysis. *Organic Geochemistry*, *62*, 28–32. https://doi.org/10.1016/j.orggeochem.2013.06.009

Wystalska, K., Malińska, K., & Barczak, M. (2021). Poultry manure derived biochars—The impact of pyrolysis temperature on selected properties and potentials for further modifications. *Journal of Sustainable Development of Energy, Water and Environment Systems*, *9*(1), 1–10. https://doi.org/10.13044/j.sdewes.d8.0337

Xiao, X., Chen, B., Chen, Z., Zhu, L., & Schnoor, J. L. (2018). Insight into multiple and multilevel structures of biochars and their potential environmental applications: A critical review. *Environmental Science and Technology*, *52*(9), 5027–5047. https://doi.org/10.1021/acs.est.7b06487

Yuan, H., Lu, T., Wang, Y., Huang, H., & Chen, Y. (2014). Influence of pyrolysis temperature and holding time on properties of biochar derived from medicinal herb (*Radix isatidis*) residue and its effect on soil CO_2 emission. *Journal of Analytical and Applied Pyrolysis*, *110*(1), 277–284. https://doi.org/10.1016/j.jaap.2014.09.016

Yuan, H., Lu, T., Zhao, D., Huang, H., Noriyuki, K., & Chen, Y. (2013). Influence of temperature on product distribution and biochar properties by municipal sludge pyrolysis. *Journal of Material Cycles and Waste Management*, *15*(3), 357–361. https://doi.org/10.1007/s10163-013-0126-9

Zhang, D., Wang, T., Zhi, J., Zheng, Q., & Chen, Q. (2020). Utilization of jujube biomass to prepare biochar by pyrolysis and activation: Characterization, adsorption characteristics, and mechanisms for nitrogen. *Materials*, *13*(24), 5594–5615. https://doi.org/10.3390/ma13245594

Zhang, H., Chen, C., Gray, E. M., & Boyd, S. E. (2017). Effect of feedstock and pyrolysis temperature on properties of biochar governing end use efficacy. *Biomass and Bioenergy*, *105*, 136–146. https://doi.org/10.1016/j.biombioe.2017.06.024

Zimmerman, A. R. (2010). Abiotic and microbial oxidation of laboratory-produced black carbon (biochar). *Environmental Science and Technology*, *44*(4), 1295–1301. https://doi.org/10.1021/es903140c

SUPPORTING INFORMATION

Additional supporting information can be found online in the Supporting Information section at the end of this article.

How to cite this article: Lebrun Thauront, J., Soja, G., Schmidt, H.-P., & Abiven, S. (2024). A critical re-analysis of biochar properties prediction from production parameters and elemental analysis. *GCB Bioenergy*, *16*, e13170. https://doi.org/10.1111/gcbb.13170